AGE (2013) 35:777–792
DOI 10.1007/s11357-012-9413-y

Cardiovascular risk in cognitively preserved elderlies is associated with glucose hypometabolism in the posterior cingulate cortex and precuneus regardless of brain atrophy and apolipoprotein gene variations

Jaqueline Hatsuko Tamashiro-Duran · Paula Squarzoni · Fábio Luís de Souza Duran · Pedro Kallas Curiati · Homero Pinto Vallada · Carlos Alberto Buchpiguel · Paulo Andrade Lotufo · Mauricio Wajngarten · Paulo Rossi Menezes · Márcia Scazufca · Tânia Corrêa de Toledo Ferraz Alves · Geraldo Filho Busatto

Received: 22 November 2011 / Accepted: 17 April 2012 / Published online: 29 April 2012

Abstract Cardiovascular risk factors (CVRF) possibly contribute to the emergence of Alzheimer's disease (AD). Fluorodeoxyglucose-positron emission tomography (FDG-PET) has been widely used to demonstrate specific patterns of reduced cerebral metabolic rates of glucose (CMRgl) in subjects with AD and in non-demented

Electronic supplementary material The online version of this article (doi:10.1007/s11357-012-9413-y) contains supplementary material, which is available to authorized users.

J. H. Tamashiro-Duran · P. Squarzoni · F. L. de Souza Duran · P. K. Curiati · T. C. de Toledo Ferraz Alves · G. F. Busatto
Laboratory of Neuroimaging in Psychiatry (LIM-21), Department of Psychiatry, University of Sao Paulo Medical School, Sao Paulo, Sao Paulo, Brazil

H. P. Vallada · M. Scazufca
Department of Psychiatry, University of Sao Paulo Medical School, Sao Paulo, Sao Paulo, Brazil

C. A. Buchpiguel
Nuclear Medicine Center, Department of Radiology, University of Sao Paulo Medical School, Sao Paulo, Sao Paulo, Brazil

P. A. Lotufo
Internal Medicine Division, University Hospital of the University of Sao Paulo, Sao Paulo, Sao Paulo, Brazil

M. Wajngarten
Heart Institute, General Hospital of University of Sao Paulo Medical School, Sao Paulo, Sao Paulo, Brazil

P. R. Menezes
Department of Preventive Medicine, University of Sao Paulo Medical School, Sao Paulo, Sao Paulo, Brazil

T. C. de Toledo Ferraz Alves
ABC Region Medical School, Sao Paulo, Sao Paulo, Brazil

J. H. Tamashiro-Duran (✉)
Centro de Medicina Nuclear, 3° andar, LIM-21, Rua Dr. Ovídio Pires Campos s/n, 05403-010 Sao Paulo, Sao Paulo, Brazil
e-mail: jhatsu@gmail.com

carriers of the apolipoprotein ε4 (APOE ε4) allele, the major genetic risk factor for AD. However, functional neuroimaging studies investigating the impact of CVRF on cerebral metabolism have been scarce to date. The present FDG-PET study investigated 59 cognitively preserved elderlies divided into three groups according to their cardiovascular risk based on the Framingham 10-year risk Coronary Heart Disease Risk Profile (low-, medium-, and high-risk) to examine whether different levels of CVRF would be associated with reduced CMRgl, involving the same brain regions affected in early stages of AD. Functional imaging data were corrected for partial volume effects to avoid confounding effects due to regional brain atrophy, and all analyses included the presence of the APOE ε4 allele as a confounding covariate. Significant cerebral metabolism reductions were detected in the high-risk group when compared to the low-risk group in the left precuneus and posterior cingulate gyrus. This suggests that findings of brain hypometabolism similar to those seen in subjects with AD can be detected in association with the severity of cardiovascular risk in cognitively preserved individuals. Thus, a greater knowledge about how such factors influence brain functioning in healthy subjects over time may provide important insigths for the future development of strategies aimed at delaying or preventing the vascular-related triggering of pathologic brain changes in the AD.

Keywords Aging · Alzheimer's disease · Positron emission tomography · Framingham Heart Study Risk Score · Apolipoprotein E

Introduction

Positron emission tomography (PET) with 18-fluoro-2-deoxyglucose (^{18}F-FDG) is currently the most accurate in vivo neuroimaging method for investigating regional brain metabolic changes associated with healthy and pathological aging in humans. Most notably, this technique has been widely applied to document regional cerebral hypometabolic changes associated with aging-related neurodegenerative disorders such as Alzheimer's disease (AD), the commonest form of dementia. In AD, consistent patterns of localized hypometabolism have been described from early disease stages, involving initially and most significantly the precuneus and posterior cingulate gyrus (Minoshima et al. 1997; Chételat et al. 2003; Mosconi 2005; Kawachi et al. 2006), and implicating also the hippocampus, amygdala, parahippocampal gyrus, and the lateral parietal and temporal neocortices (Mosconi et al. 2004, 2008a; Jagust 2006; Petrie et al. 2009). There have also been PET studies documenting regional brain glucose metabolism variations as a function of the apolipoprotein E (APOE) genotype in non-demented individuals, with glucose hypometabolism being associated with the presence of the APOE ε4 allele (Drzezga et al. 2005; Mosconi et al. 2008b; the major genetic risk factor for AD; Corder et al. 1993).

Cardiovascular risk factors (CVRF), such as hypertension, diabetes, dyslipidemia, and smoking, are highly prevalent in the elderly population and have a significant impact on cognitive performance (Obisesan et al. 2008; Fitzpatrick et al. 2009; Li et al. 2011). Such conditions are nowadays recognized as risk factors not only for vascular dementia but also for AD (Launer et al. 2000; Meyer et al. 2000; Knopman et al. 2001; Stuerenburg et al. 2005; Rosendorff et al. 2007; Irie et al. 2008; Xu et al. 2009). There are also findings from post mortem and in vivo morphometric magnetic resonance imaging (MRI) studies indicating that brain lesions of vascular origin, such as white matter hyperintensities, stroke, and lacunar infarcts, may be significantly associated with AD (Craft 2009; Erkinjuntti and Gauthier 2009; Teipel et al. 2009). Moreover, the presence of the APOE ε4 allele is an important risk factor not only for AD but also for cardiovascular disease (Irie et al. 2008; Kivipelto et al. 2008). Such body of evidence has led to propositions that vascular-related mechanisms possibly play a critical role in the pathophysiology of AD (de la Torre and Mussivand 1993; de la Torre 2009; Qiu et al. 2009; Viswanathan et al. 2009).

Studies assessing non-demented individuals with high levels of CVRF using FDG-PET may provide further support to the "vascular hypothesis" for AD, particularly if localized brain functional changes in such subjects can be detected in the same brain regions known to be primarily affected in AD. In the only large FDG-PET study that investigated such issue to date, Reiman et al. (2010) searched for significant associations between serum total cholesterol levels and cerebral metabolic rates of glucose (CMRgl) in 117 cognitively normal middle-aged and elderly individuals (47 to 68 years of age). The sample was subdivided in APOE ε4 allele homozygotes (n=24), heterozygotes (n=38), and non-carriers of this genetic variant (n=55). Higher serum total cholesterol levels were associated with

lower CMRgl bilaterally in the precuneus, lateral parietal neocortex (encompassing the superior parietal lobule, angular and supramarginal gyri), lateral temporal neocortex (involving the superior temporal gyrus), and lateral prefrontal cortex (including the superior frontal gyrus), in a pattern that shows a substantial degree of overlap with the profile of regional brain functional changes commonly seen in subjects with mild AD (Reiman et al. 2010). Moreover, these authors found that in some cortical regions, such relationship had greater salience in APOE ε4 allele carriers than in non-carriers. They postulated that higher cholesterol levels, particularly in association with the presence of the APOE ε4 allele, increase the risk of AD by accelerating some of the brain changes associated with normal aging (Reiman et al. 2010).

In additional studies with more modest samples, findings of regional cerebral hypometabolism as assessed with FDG-PET have been described in association with other CVRF including insulin resistance (Baker et al. 2011), obesity (Volkow et al. 2009), and elevated blood pressure (Langbaum et al. 2012). These studies have described significant associations between those risk factors and reduced brain glucose metabolism, variably implicating the precuneus, posterior cingulate gyrus, lateral parietal neocortex, and lateral temporal neocortex (Baker et al. 2011; Langbaum et al. 2012), as well as the lateral prefrontal cortex (Volkow et al. 2009; Langbaum et al. 2012).

CVRF rarely occur in isolation in elderly populations (Meigs et al. 1997; Razay et al. 2007), and therefore, the approach of investigating the influence of single risk factors on brain glucose metabolism may be limited. The Framingham 10-year risk Coronary Heart Disease Risk Profile [FCHDRP (10-year risk)] is a composite measure that takes into account multiple risk factors (such as age, gender, blood pressure, smoking status, total cholesterol, and high-density lipoprotein cholesterol levels, as well as the presence of diabetes) to assess the 10-year risk that an individual has for future coronary heart disease (Wilson et al. 1998). This risk score has been widely used in epidemiological studies of elderly populations (Jeerakathil et al. 2004; Seshadri 2006). In the only FDG-PET study to date that used this strategy, Kuczynski et al. (2009) obtained measures of regional glucose metabolism and cardiovascular risk as assessed with the FCHDRP (10-year risk) in a relatively large sample of elderly subjects (n=58; age, >55 years), focusing specifically on the frontal lobe. These authors observed a significant inverse association between FCHDRP (10-year risk) scores and CMRgl in different frontal lobe portions including the lateral (i.e., superior frontal gyrus and ventrolateral prefrontal cortex) and medial (i.e., superior medial frontal and superior orbital frontal gyri) prefrontal cortices (Kuczynski et al. 2009). However, it is difficult to interpret such findings as related specifically to functional deficits caused by direct effects of CVRF on the brain, as the study sample included a proportion of demented individuals in addition to healthy elderlies, and no assessment of the impact of the APOE ε4 allele was carried out.

With the aim of extending the above findings, we conducted a FDG-PET investigation in a sample of elderly subjects free of either dementia or milder forms of cognitive impairment, subdivided in three groups according to their degree of cardiovascular risk as assessed by FCHDRP (10-year risk) scores. We wished to test the hypothesis that an elevated FCHDRP (10-year risk) would be associated with hypometabolism in brain regions commonly implicated in the pathophysiology of AD, namely the precuneus, posterior cingulated gyrus, amygdala–hippocampus complex, parahippocampal gyrus, and lateral temporal and parietal neocortices. Also, we wished to investigate whether such associations would be present regardless of the presence of the APOE ε4 allele. Finally, as the above functional imaging literature has often suggested the presence of prefrontal hypometabolism in association with CVRF (Kuczynski et al. 2009; Volkow et al. 2009; Langbaum et al. 2012), we also hypothesized the presence of CVRF-related brain functional deficits in the lateral prefrontal and medial prefrontal cortices.

Materials and methods

All study procedures were approved by the local Committee for Ethics and Research, and written informed consent was obtained from all participants prior to study enrollment.

Study sample and clinical features

This study was carried out in a subsample drawn from a pool of 248 non-demented elderly volunteers (age range, 66–75 years) recruited for a previously reported morphometric MRI study aimed at investigating gray matter volume changes associated with different levels

of CVRF (de Toledo Ferraz Alves et al. 2011). Such pool of 248 individuals was representative, in terms of their sociodemographic profile, of a population of subjects aged 65 or above (n=2,072) of pre-defined census sectors of an economically disadvantaged area of São Paulo, Brazil. This population was identified by epidemiological investigation carried out in Brazil (Scazufca et al. 2008b), the São Paulo Ageing and Health study (SPAH), with the primary purpose of determining the prevalence of dementia and its risk factors in that environment, using transcultural protocols developed by the 10/66 Dementia Research Group (Prince et al. 2007; Scazufca and Seabra 2008a; Scazufca et al. 2008b).

The procedures for the selection of the 248 individuals who underwent MRI scanning from the pool of 2,072 subjects have been described in detail elsewhere (de Toledo Ferraz Alves et al. 2011). In brief, information on participants' age was obtained by asking dates of birth and confirmed from identity cards. The presence of diabetes mellitus was defined by a fasting blood glucose level ≥126 mg/dl and/or current use of insulin or hypoglycemic oral drug treatment. Levels of total cholesterol and total high-density lipoprotein (HDL) were obtained using the cholesterol-oxidase method. Three measurements of blood pressure were performed with an OMRON digital sphygmomanometer, model HEM-712-C. Measurements were taken at least 1 h without ingestion of caffeine and/or smoking, with participants seated. The first measurement was taken after 5 min of rest, and the two remaining measurements were taken at intervals of 5 min. For the calculation of the arterial pressure value, the first measurement was discarded, and the arithmetic mean of the second and third measurements was calculated. Finally, participants were asked about their smoking habits. The FCHDRP (10-year risk) calculated for each subject was then used in order to subdivide the sample in the following three groups according to their risk angina or myocardial infarction: low (<10 %), medium (10 to 20 %), and high (>20 %). In this total sample (n=248), we found no subjects with a diagnosis of atrial fibrillation based on electrocardiogram examinations.

The following exclusion criteria were applied for the selection of the pool of 248 non-demented elderly subjects who underwent MRI scanning: all individuals aged above 75 years at time of recruitment for MRI scanning (n=996), as well as those who had either not completed the 2-year clinical follow-up, present any missing data that prevented FCHDRP (10-year risk) scoring (n=107), or who fulfilled diagnostic criteria for neuropsychiatric disorders (n=52). This led to the identification of 917 potentially eligible individuals who were classified in terms of their cardiovascular risk according to the FCHDRP (10-year risk) in low-risk (24 %), medium-risk (36.4 %), and high-risk (39.1 %) subjects. Telephone contacts were then made with each potentially eligible subject in order to invite him or her to take part in the brain imaging study, and to check for the presence of contraindications for MRI scanning (carrying cardiac pacemaker, valvular prosthesis, or internal electrical magnetic device; history of neurosurgery; or presence of metal fragment in brain, eye, or spinal cord). We were unable to contact 103 subjects, and for those who were reachable, the number of exclusion was 206 subjects (132/74, female/male) who fulfilled the exclusion criteria for the study (presence of cognitive decline, mild cognitive impairment, dementia history of stroke, epilepsy, brain trauma, and transitory ischemic event), thus resulting in a total of 608 potential subjects to be invited to undergo the brain imaging session. Finally, considering the possibility of several subjects with silent brain lesions, MRI scan was performed in 248 dementia-free elderly subjects aged between 66 and 75 years [female/male (134/114)] divided according to cardiovascular risk scanning [low-risk (n=58), medium-risk (n=88), and high-risk (n=102)] in order to guarantee the statistical power.

The identification of cases of dementia and other major psychiatric disorders by the epidemiological team followed the protocol developed by the 10/66 Dementia Research Group (Prince et al. 2007; Scazufca and Seabra 2008a; Scazufca et al. 2008b). This protocol included the Community Screening Instrument for Dementia (CSI-D), the Geriatric Mental State (GSM), a structured neurological assessment, and a structured cardiological evaluation. The CSI-D affords an item-weighted summary score (COGSCORE) from the participant's 32-item cognitive test (seven-item object denomination, four-item object definition, two verbal category fluency tasks, word repetition, identification of a famous person, temporal and spatial orientation, three orders, three-word recall, six-chunk story recall, and two drawings of intersecting circles and pentagons), also incorporating the Consortium to Establish a Registry for Alzheimer's Disease (CERAD) animal-naming verbal fluency task and the modified CERAD ten word

list learning task with delayed recall (Copeland et al. 1986). The protocol also had specific questions regarding Parkinson's disease, epilepsy, symptomatic or transient ischemic attacks, and severe head trauma. The criterion for the exclusion of subjects with mild cognitive impairment, after excluding cases of dementia, was defined as a performance of 1.5 standard deviation below the mean performance in the cognitive battery described above obtained from all subjects between 66 and 75 years of age from the original SPAH sample. Schooling data of each subject was extracted from the SPAH study database. In brief, we considered subjects as having 4 years of education if they had completed the fourth grade, 8 years if having completed the eighth grade, 11 years if having completed high school, and 15 years if having completed college. When one of these educational periods was not completed, the number of years until drop out was used as the estimate of mean number of years of education.

For the current PET study, we planned to obtain a sample of 60 cognitively intact elderly subjects by consecutively inviting through phone calls the volunteers that had been recruited for the above-cited MRI study, with an aim of obtaining a minimum of 15 subjects in each of the three groups divided according to their FCHDRP (10-year risk). We excluded from the list of potential subjects for the current study any individuals presenting diabetes mellitus, given the potential of this disorder to significantly alter the brain FDG-PET measures (Vander Borght et al. 2001; Bartenstein et al. 2002), and subjects who had silent brain lesions identified at MRI scanning, including tumors and silent brain infarcts. The recruitment procedures were halted when 60 eligible individuals had been selected for FDG-PET imaging. The estimate of 60 subjects was based on statistical power calculations performed using the software G*Power3 (Faul et al. 2007; Eriksson et al. 2009), in order to attain a power of 0.80 with an α error probability of 0.05 and effect size of 0.40 to unravel CMRgl differences across the three groups. One subject was excluded because of motion artifact in PET brain imaging, resulting in a final sample of 59 subjects. This group showed a similar distribution in terms of mean age, gender, and mean years of education relative to the larger pool of 248 individuals selected for the larger MRI study. The proportion of subjects across the three groups divided according to their cardiovascular risk was as follows: low-risk (n=18), medium-risk (n=21), and high-risk (n=20).

Genotyping: APOE ε4 allele measures

For two out of the 59 individuals above (one in the low-risk group, one in the medium-risk group), APOE genotyping was not available, resulting in a sample of 57 subjects for the analyses taking into account this variable. Genomic deoxyribonucleic acid (DNA) was extracted from EDTA-anticoagulated venous blood using standard salting-out method. The concentration of extracted DNA was determined by spectrophotometric measurements. Five microliters of the extracted DNA was diluted 1:50 in 0.2× TE buffer. Absorption was measured for both blank (only 0.2× TE) and diluted DNA solutions at 260 nm using the GeneQuant (Amersham Pharmacia). An absorbance (A260) of 1.0 corresponds to 50 μg of double-stranded DNA per milliliter. After quantification, the DNA was diluted to a working level of 10 ng/μL. The single nucleotide polymorphisms (SNPs) rs429358 and rs7412 that determine the three APOE isoforms (APOE2, APOE3, and APOE4) were used to genotype all subjects under contract by Prevention Genetics (www.preventiongenetics.org) using the Amplifluor SNPs genotyping system (Chemicon International, Temecula, CA, USA). Tests for deviation from the Hardy–Weinberg equilibrium were performed for the whole sample of the SPAH. The two loci were tested and did not deviate from the Hardy–Weinberg equilibrium.

In regard to quality control procedures, the genotyping of all individuals was performed in the laboratory of Genetics and Pharmacogenetics Program (PROGENE, Department of Psychiatry, São Paulo University Medical School) before sending the samples to Prevention Genetics. The degree of discrepancy between this genotyping and the one carried out by Prevention Genetics was below 2 %, and we report herein the results obtained in the analysis carried out by Prevention Genetics. We considered positive to APOE4 status as the presence of at least one allele ε4 in the genotype, including both heterozygous and homozygous carriers.

Brain imaging data acquisition and reconstruction

MRI data were acquired using a 1.5-T General Electric Signa LX CVi scanner (Milwaukee, WI, USA). The standardized acquisition protocols have been described in detail elsewhere (de Toledo Ferraz Alves et al. 2011).

On average, FDG-PET examinations were carried out 11.17±7.15 months after the acquisition of MRI data. At the time of PET scanning, all returning

subjects were re-examined and remained cognitively intact. There were no significant differences in the mean time intervals between the FDG-PET and MRI examinations across the three groups (p=0.596). PET images were acquired by using a dedicated lutetium oxyorthosilicate-16-slice PET-CT scanner (Biograph-16, Siemens, Erlangen, Germany) with a spatial resolution of 2.5 mm full-width at half-maximum (FWHM), 3.38 mm slice thickness, and 500 mm axial FOV, following exactly the same protocol reported in detail elsewhere (Curiati et al. 2011).

Image preprocessing and processing

When registering FDG-PET images of an individual to his own MRI data, the former functional images often contain little non-brain tissue because of the nature of the imaging process, whereas the high-resolution MRI scans contain a considerable amount of extracerebral tissue (i.e., eyeballs, skin, and fat). Thus registration robustness is improved if these non-brain parts of the image can be automatically removed before registration (Smith et al. 2001, 2002).

A recent study of Pereira et al. (2010) showed that preprocessing (skull-stripped/bias corrected scans) of brain MRI datasets, especially in studies based on voxel-based morphometry to investigate the process of aging and dementia, improved voxel-based morphometry outputs. We therefore performed our experiments with the same preprocessing steps as described previously (Acosta-Cabronero et al. 2008; Pereira et al. 2010). Regarding PET data, all images were corrected for partial volume effects (PVE) to avoid confounding effects secondary to the degree of regional brain atrophy. The correction for the dilutional effect of age-related cerebral atrophy is mandatory in PET brain evaluations and may play an important role in the differentiation between normal and pathological brain changes associated with the aging processes (Meltzer et al. 2000). Thus, the co-registered PET images were corrected for PVE through the Meltzer method, an optimized voxel-based algorithm that is fully implemented in PVElab software (http://nru.dk/downloads/softaware) (Quarantelli et al. 2004).

The procedure has been specifically designed for this study, aiming at a most accurate co-processing of FDG-PET and MRI data to obtain a more precise between-subject anatomical overlap. All image-processing steps were carried out using the SPM5 software package (Statistical Parametric Mapping software, version 5; http://www.fil.ion.ucl.ac.uk/spm; Wellcome Department of Imaging Neuroscience, London) executed in Matlab 7.8 (MathWorks Inc., Sherborn, MA, USA). Additional details are provided in the Online Resource 1.

Statistical analysis

Statistical comparisons of the three FCHDRP (10-year risk) groups (low-risk, medium-risk, and high-risk) in terms of demographic and clinical characteristics (including genotype measures) were performed using the Statistical Package for Social Sciences (SPSS) for Windows (17.0 version). Chi-square tests were used for categorical variables, whereas analyses of variance (ANOVA) were carried out for continuous variables. Levels of statistical significance were set at $p<0.05$.

Group comparisons of PET images were conducted using SPM5. Between-group differences in CMRgl distribution across the three FCHDRP (10-year risk) groups were assessed initially with an overall analysis of covariance (ANCOVA) model, including gender and the mean time interval between the FDG-PET and MRI data acquisitions for each individual as covariates of no interest. Resulting statistics were thresholded at a two-tailed $p<0.01$ level of significance ($Z>2,33$) and displayed as a statistical parametric map into standard anatomical space. The ANCOVA SPM was inspected on a hypothesis-driven fashion, searching for clusters of voxels in regions where between-group differences had been predicted a priori (amygdala, hippocampus, parahippocampal gyrus, precuneus, posterior cingulate gyrus, lateral temporal and parietal neocortices, and lateral and medial prefrontal cortices. This hypothesis-driven analysis was conducted using the small volume correction (SVC) approach, with the purpose of constraining the total number of voxels to be inspected. Each of those regions was circumscribed using the spatially normalized region-of-interest masks that are available within the Anatomical Automatic Labeling SPM toolbox. All findings in those areas were reported as significant only if surviving family-wise error (FWE) correction for multiple comparisons using SVC (Friston et al. 1996). Given that the F statistic is non-directional, we also conducted voxelwise two-group comparisons of CMRgl differences in these regions using independent sample t tests. In addition to the hypothesis-driven SPM inspection, we conducted a whole-brain search for significant findings in other unpredicted brain regions.

Such findings were reported as significant only if surviving FWE correction for multiple comparisons over the whole brain ($p_{FWE}<0.05$) (Friston et al. 1996). We also calculated voxelwise linear correlation indices between CMRgl values and FCHDRP (10-year risk) scores using the entire sample of elderly individuals. SVC-based correlation analyses were conducted using the same anatomical masks described above.

Finally, in order to assess the impact of APOE genotype variations on our findings of voxel-based analyses, we repeated the above analysis including the presence or absence of the APOE ε4 allele as a confounding covariate of interest.

The anatomic location of each resulting cluster was determined using the Talairach and Tournoux Atlas coordinates (Talairach and Tournoux 1988), converted from the Montreal Neurological Institute (MNI) system (Brett et al. 2002).

Results

Demographic and clinical characteristics of the sample

Table 1 presents the demographic and clinical characteristics for the whole sample ($n=59$). We noted a gender imbalance across the three groups ($p=0.003$), with a predominance of women in the low-risk cardiovascular risk group and a greater prevalence of men in the high-risk group. There were no significant between-group differences in regard to age, mean years of education, and smoking. However, as expected, there were significant group differences in terms of low-density lipoprotein (LDL) and HDL cholesterol levels ($p=0.044$ and $p=0.046$, respectively), systolic and diastolic blood pressures ($p<0.001$ and $p=0.002$, respectively), and blood glucose levels ($p=0.048$).

Cognitive performance comparisons between the three groups showed no significant findings either in regard to the overall COGSCORE (low-risk=30.19±2.21, medium-risk=30.23±1.30, and high-risk=30.07±2.74) or to scores specifically in the animal-naming fluency task (low-risk=15.44±4.79, medium-risk=16.24±4.66, and high-risk=14.05±3.94; $F<1.86$, $p>0.165$).

The APOE ε4 allele was found in 11 subjects (all ε4 heterozygotes). We did not observe significant differences in APOE ε4 allele prevalence across the three groups (low-risk=3, medium-risk=6, and high-risk=2; $\chi^2=2.61$, $df=2$, $p=0.271$).

A similar pattern of between-group sociodemographic and clinical differences emerged when inspecting the three groups after the exclusion of the two individuals with missing APOE genotype data. A gender imbalance was maintained across the three groups [low-risk (W: women/M: men), 11/6; medium-risk, 10/10; and high-risk, 2/18; $\chi^2=12.62$, $df=2$, $p=0.002$]. There were significant group differences in terms of LDL cholesterol levels ($F=3.226$, $p=0.047$), and systolic and diastolic blood pressures ($F=9.494$, $p<0.001$ and $F=6.059$, $p=0.004$, respectively). There were also

Table 1 Demographic and clinical characteristics of the study groups divided according to their cardiovascular risk using the Framingham 10-year Coronary Heart Disease Risk Profile

	Low-risk ($n=18$)	Medium-risk ($n=21$)	High-risk ($n=20$)	Statistical value	p
Mean age (±SD) in years	72.01 (±2.68)	71.62 (±2.39)	72.78 (±2.75)	1.05[a]	0.358
Male (%)/female (%)	7 (38.9)/11 (61.1)	11 (52.4)/10 (47.6)	18 (90.0)/2 (10.0)	11.43[b]	0.003
Mean years of education (±SD)	5.44 (±3.94)	5.57 (±3.56)	4.10 (±3.42)	1.01[a]	0.372
Smoking (%)	1 (5.6)	5 (23.8)	4 (20.0)	2.49[b]	0.287
LDL cholesterol (±SD)	106.72 (±23.29)	117.48 (±36.92)	131.55 (±26.79)	3.30[a]	0.044
HDL cholesterol (±SD)	64.22 (±13.29)	54.38 (±14.88)	54.45 (±12.32)	3.27[a]	0.046
Systolic BP (±SD)	127.33 (±18.03)	148.14 (±31.18)	163.70 (±21.68)	10.38[a]	<0.001
Diastolic BP (±SD)	78.83 (±9.08)	83.14 (±12.02)	92.08 (±11.88)	7.06[a]	0.002
Blood glucose (±SD)	95.00 (±9.85)	101.00 (±9.43)	103.60 (±12.42)	3.21[a]	0.048

LDL low-density lipoprotein, *HDL* high-density lipoprotein, *BP* blood pressure, *SD* standard deviation

[a] ANOVA

[b] χ^2

trends for between-group differences in regard to HDL cholesterol (F=3.042, p=0.056) and blood glucose levels (F=3.070, p=0.055).

FDG-PET imaging findings: voxelwise between-group CMRgl comparisons and linear correlations

The ANCOVA investigation of CMRgl differences across the three groups showed a trend towards significance in one of the regions where differences in FDG uptake had been predicted a priori, namely the right lateral parietal neocortex (cluster of 129 voxels, Z=3.49, p_{FWE}=0.075). Independent sample t tests comparing groups two-by-two revealed several clusters of between-group differences. These findings are reported in detail in Table 2. In comparison to the low-risk group, the high-risk group presented significant CMRgl reductions in the right lateral parietal neocortex (p_{FWE}=0.027), the left precuneus (p_{FWE}=0.012), the right and left posterior cingulate gyrus (p_{FWE}=0.018 and p_{FWE}=0.004), and the right lateral temporal neocortex (p_{FWE}=0.022; Table 2). There was also an unexpected focus of significant CMRgl reduction in the low-risk group relative to the high-risk group in the right parahippocampal gyrus (p_{FWE}=0.031; Table 2). There were no significant findings in the t test comparisons of the medium-risk group versus either the high- or low-risk samples in the hypothesized regions. Also, there were no significant findings in the exploratory inspection of other unpredicted brain regions.

Finally, the voxelwise linear correlation analysis between CMRgl values and FCHDRP (10-year risk) scores for the whole sample revealed the presence of foci of significant positive correlation involving the parahippocampal gyrus, both on the right (p_{FWE}=0.022) and left (p_{FWE}=0.034) sides (Table 2).

PET data analyses with covariance for the presence or absence of the APOE ε4 allele

When the above analyses were repeated including the presence or absence of the APOE ε4 allele as covariate, the ANCOVA investigation of CMRgl differences across the three groups showed also an unexpected focus of

Table 2 Hypothesis-driven search for significant between-group differences in CMRgl distribution across the three FCHDRP (10-year risk) groups and linear correlations between CMRgl values and FCHDRP (10-year risk) scores in the overall sample of elderly subjects (n=59, including gender and mean time interval between MRI and FDG-PET data acquisitions as covariates of no interest)

Region name (SVC)[a]	Hemisphere	Brodmann areas	K[b]	$p_{FWE\text{-}corrected}$[c]	T[d]	Z[e]	$p_{uncorrected}$[f]	Coordinates x, y, z[g]
Significant CMRgl reduction in low-risk group in comparison to high-risk group								
Parahippocampal gyrus	Right	36	50	0.031	3.59	3.28	0.001	30, −30, −14
Significant CMRgl reductions in high-risk group in comparison to low-risk group								
Lateral parietal neocortex	Right	39/40	240	0.027	4.25	3.78	<0.001	44, −59, 31
Precuneus	Left	7/23/31	458	0.012	4.37	3.86	<0.001	−6, −43, 37
Posterior cingulate gyrus	Right	7/23/31	22	0.018	3.41	3.14	0.001	2, −49, 30
	Left	7/23/31	91	0.004	4.09	3.66	<0.001	−4, −47, 32
Lateral temporal neocortex	Right	19/22/39/40	12	0.022	4.44	3.92	<0.001	50, −55, 23
Significant positive correlation between CMRgl values and FCHDRP (10-year risk) scores								
Parahippocampal gyrus	Right	36	67	0.022	3.57	3.37	<0.001	30, −30, −14
	Left	36	73	0.034	3.33	3.17	0.001	−26, −32, −14

CMRgl cerebral metabolic rate for glucose metabolism, *FCHDRP* (*10-year risk*) Framingham 10-year risk Coronary Heart Disease Risk Profile, *MRI* magnetic resonance imaging, *FDG-PET* positron emission tomography with 18-fluoro-2-deoxyglucose

[a] Each region was circumscribed using the small volume correction (SVC) approach, with anatomically defined volume-of-interests masks

[b] Number of contiguous voxels that surpassed the initial threshold of p<0.01 (uncorrected) in the statistical parametric maps

[c] Statistical significance after correction for multiple comparisons; inferences made at the level of individual voxels [family-wise error correction (FWE; Friston et al. 1996)]

[d] T-score value of statistical significance level in the cluster

[e] Z-score value of statistical significance level in the cluster

[f] Statistical significance level uncorrected for multiple comparisons

[g] Talairach and Tournoux (1988) coordinates of the maximal statistical significance within each cluster

significant CMRgl reduction in the right parahippocampal gyrus (p_{FWE}=0.032). In the two-group comparisons, significant CMRgl reductions were detected in the high-risk group compared to the low-risk group in the left precuneus (p_{FWE}=0.008) and the left posterior cingulate gyrus (p_{FWE}=0.007; see Table 3 for details); these findings are shown in Fig. 1. The above reported, unexpected foci of CMRgl reductions in the low- compared to the high-risk group in the parahippocampal gyrus was again detected, both on the right (p_{FWE}=0.001) and left (p_{FWE}=0.045) hemispheres. The significant positive linear correlation between CMRgl values and FCHDRP (10-year risk) scores in the parahippocampal gyrus also retained statistical significance both for the right (p_{FWE}= 0.007) and left (p_{FWE}=0.025) sides (Table 3).

Discussion

Using a sample of cognitively intact community-dwelling elderly subjects, the present FDG-PET study demonstrated the presence of reduced glucose metabolism in the precuneus, posterior cingulate gyrus, and lateral temporal and parietal neocortices in proportion to the degree of cardiovascular risk as measured with the most extensively validated composite index devised for such purpose, namely the FCHDRP (10-year risk) score. Our hypothesis that CVRF-related reduced brain glucose metabolism would be detected specifically in these brain portions was formulated with basis on a large number of previous PET studies of AD, which demonstrated the presence of significantly impaired functional activity in such network of brain regions (Minoshima et al. 1997; Chételat et al. 2003; Mosconi et al. 2004, 2008a; Mosconi 2005; Jagust 2006; Kawachi et al. 2006; Petrie et al. 2009). Thus, our FDG-PET findings provide further evidence indicating that there is a substantial degree of overlap in regard to the location of brain foci of hypofunction across imaging studies of AD and CVRF (Alves et al. 2005; Kuczynski et al. 2009; Volkow et al. 2009; Kitagawa 2010; Reiman et al. 2010; Baker et al.

Table 3 Hypothesis-driven search for significant between-group differences in CMRgl distribution across the three FCHDRP (10-year) groups and linear correlations between CMRgl values and FCHDRP (10-year) scores in the sample of elderly subjects (n=57, including gender and mean time interval between MRI and PET data acquisitions as covariates of no interest), controlling to APOE ε4 status

Region name (SVC)[a]	Hemisphere	Brodmann areas	K[b]	$p_{FWE\text{-corrected}}$[c]	F/T[d]	Z[e]	$p_{uncorrected}$[f]	Coordinates x, y, z[g]
Significant CMRgl difference in comparisons across the three groups: low-risk, medium-risk, and high-risk								
Parahippocampal gyrus	Right	35/36	34	0.032	9.00	3.32	<0.001	32, −26, −17
Significant CMRgl reduction in low-risk group in comparison to high-risk group								
Parahippocampal gyrus	Right	35/36	133	0.001	5.08	4.32	<0.001	32, −26, −17
	Left	35/36	66	0.045	3.38	3.10	0.001	−26, −30, −15
Significant CMRgl reductions in high-risk group in comparison to low-risk group								
Precuneus	Left	7/23/31	401	0.008	4.60	4.00	<0.001	−6, −43, 37
Posterior cingulate gyrus	Left	23/31	71	0.007	3.89	3.50	<0.001	−4, −47, 32
Significant positive correlation between CMRgl values and FCHDRP (10-year risk) scores								
Parahippocampal gyrus	Right	35/36	114	0.007	4.00	3.72	<0.001	30, −30, −14
	Left	35/36	95	0.025	3.47	3.27	0.001	−26, −32, −14

CMRgl cerebral metabolic rate for glucose metabolism, *FCHDRP* (*10-year risk*) Framingham 10-year risk Coronary Heart Disease Risk Profile, *MRI* magnetic resonance imaging, *FDG-PET* positron emission tomography with 18-fluoro-2-deoxyglucose

[a] Each region was circumscribed using the small volume correction (SVC) approach, with anatomically defined volume-of-interests masks

[b] Number of contiguous voxels that surpassed the initial threshold of p<0.01 (uncorrected) in the statistical parametric maps

[c] Statistical significance after correction for multiple comparisons; inferences made at the level of individual voxels [family-wise error correction (FEW; Friston et al. 1996)]

[d] F or T-score value of statistical significance level in the cluster

[e] Z-score value of statistical significance level in the cluster

[f] Statistical significance level uncorrected for multiple comparisons

[g] Talairach and Tournoux (1988) coordinates of the maximal statistical significance within each cluster

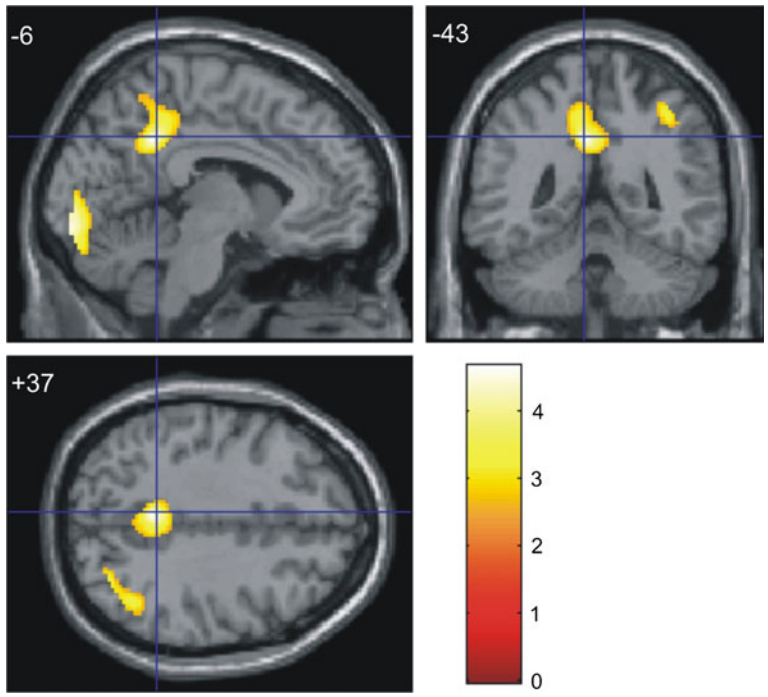

Fig. 1 Brain pattern of reduced FDG uptake in the high-risk group in comparison to the low-risk group. Results of the whole-brain search of significant cerebral metabolic rate for glucose metabolism reductions in the high-risk group (n=20) in comparison to the low-risk group (n=17), controlled to apolipoprotein ε4 status (at the Z>2.33 threshold, corresponding to p<0.01). Foci of significance were overlaid on sagittal (x), coronal (y), and transaxial (z) brain slices of a structural magnetic resonance imaging scan spatially transformed into an approximation to the Talairach and Tournoux (1988) stereotactic atlas with a *cross hair* marking the location of the average peak coordinate as *indicated by numbers* (x=−6, y=−43, y=+37) in millimeters. Statistical voxel values have been thresholded at Z=2.33 (corresponding to p<0.01, uncorrected for multiple comparisons). The brain regions where hypoactivity (clusters *highlighted in yellow*) in the high-risk group had been hypothesized a priori, and which showed significant differences between the two groups (at the 0.05 level after family-wise error correction for multiple comparisons, using the small volume correction tool in Statistical Parametric Mapping), were the left precuneus and the left posterior cingulate gyrus. The coordinates of voxels of maximal statistical significance in each cluster, as well as their size, peak Z-scores, and associated p values, are provided in Table 3. The *color bar* represents T-values

2011; Langbaum et al. 2012). As the present study sample was carefully screened for the exclusion of cognitive decline, our results suggest that cognitive deficits do not necessarily accompany brain metabolic deficits reminiscent of AD in individuals who are at large cardiovascular risk. Our findings add to evidence from previous epidemiological and morphometric MRI studies that have assessed non-demented individuals using FCHDRP (10-year risk) indices (Massaro et al. 2004; Seshadri et al. 2004; de Toledo Ferraz Alves et al. 2011), thus providing further support to the notion that different CVRF, acting in combination, may play a relevant part in the development of AD (Gorelick 2004; Erkinjuntti and Gauthier 2009; Viswanathan et al. 2009).

In the larger MRI study sample of cognitively intact elderly subjects from which the current PET groups were drawn, findings of decreased regional brain volumes were also detected in direct proportion to the degree of cardiovascular risk. Such previously reported brain volume changes were localized to the temporal neocortex, in similar locations where temporal lobe functional deficits were detected herein (de Toledo Ferraz Alves et al. 2011). In the present PET study, we employed image-processing methods to account for partial volume effects due to local brain atrophy. Therefore, our PET findings in the temporal neocortex can be safely assumed to represent true metabolic deficits, found in excess of any brain tissue reduction in the same brain location. It is also interesting that the current FDG-PET findings of reduced FDG uptake in proportion to the degree of cardiovascular risk were more extensively distributed that those described in our previous MRI report (de Toledo Ferraz Alves et al. 2011), despite the fact that

the present sample was more modest in size. This suggests that FDG-PET may unravel CVRF-related localized brain metabolic deficits in brain regions related to AD before any subtle brain atrophic changes can be detected in cognitively preserved individuals.

After controlling for the presence of the APOE ε4 allele, a critical genetic risk factor for both AD and cardiovascular disease, our findings of CVRF-related regional brain hypofunctional patterns retained statistical significance in the precuneus and posterior cingulate gyrus, the two brain regions where functional impairments are most consistently detected in incipient stages of AD (Minoshima et al. 1997; Chételat et al. 2003; Mosconi 2005; Kawachi et al. 2006). This strongly suggests that findings of brain hypometabolism similar to those seen in AD subjects can be seen in association with the severity of CVRF in samples of cognitively preserved individuals who are at no increased genetic risk for AD (as far as the APOE genotype is concerned). Other findings of reduced FDG uptake in the high-risk group, involving the lateral temporoparietal neocortices, lost their significance when the analysis was repeated after controlling for the effects of the presence of the APOE ε4 allele. This may indicate that findings of reduced FDG uptake in those latter regions are primarily influenced by the presence of the APOE ε4 allele, as suggested by previous PET studies of non-elderly, cognitively preserved healthy subjects (Reiman et al. 2004, 2010; Langbaum et al. 2010). One alternative interpretation is that such absence of significance was related to reduced statistical power due to the loss of 1° of freedom and/or the decrement of the sample size (as there were missing APOE genotype data in two subjects).

Several different mechanisms have been proposed to explain how microvascular mechanisms could contribute critically to the development and/or progression of AD-related pathological changes in the brain. Previous results from clinical imaging and molecular studies have suggested a link between CVRF, structural deformities of brain microvessels (including arterial stiffness and microvascular damage), and the risk of dementia (Bell et al. 2009; Grammas 2011a). Chronic cerebral blood flow deficits secondary to conditions such as diabetes, hypertension, and atherosclerosis, as well as heart failure-related microembolism, may all lead to decreased oxygen and glucose supply to the brain, as well as local toxic or metabolic disturbances (Kumar-Singh 2008; Bangen et al. 2009; Menon and Kelley 2009). It has been suggested that microvascular changes secondary to chronic cerebral blood flow reductions might trigger the characteristic neuropathological changes of AD, such as aggregates of amyloid β-peptide (de la Torre 1999; de la Torre et al. 2003). Recently, molecular models have been proposed to explain how the existence of circulatory defects (i.e., alterations in vascular smooth muscle cells of meningeal arterioles due to CVFR) could lead to a failure in an essential brain detoxification process, namely the removal of amyloid β-peptide from the brain across the blood–brain barrier (Bell et al. 2009). Finally, the endothelium is also a potentially relevant target for the damaging effects of CVRF, and it has been shown that functional impairment of the vascular endothelium in response to injury occurs long before the development of overt cardiovascular disease (Gimbrone 1999, 2010; Libby 2009). Chronic inflammatory processes, tightly linked to diseases associated with endothelial dysfunction, have been increasingly implicated as relevant to the development of the neurodegenerative changes underlying the symptoms of AD (Grammas 2000; Zlokovic 2005, 2010; Salmina et al. 2010; Grammas et al. 2011b).

It should be noted that we found no association between high cardiovascular risk and brain functional deficits specifically in the frontal cortex. This is in contrast both with the recently reported findings of cardiovascular risk-related prefrontal hypofunctioning in elderly subjects classified using the FCHDRP (10-year risk) (Kuczynski et al. 2009), and the results of other PET imaging studies that investigated the influence of single CVRF on brain functioning (Baker et al. 2011; Reiman et al. 2010; Volkow et al. 2009; Langbaum et al. 2012). One important difference between our study and that of Kuczynski et al. (2009) is that the latter authors did not exclude subjects with lacunar infarcts. They actually suggested that findings of frontal lobe hypometabolism in individuals with higher FCHDRP (10-year risk) scores could be determined by the greater incidence of lacunar infarcts in those subjects, leading to localized frontal metabolic changes. This reasoning might explain the absence of frontal metabolic changes in our study, since we excluded subjects with vascular-related silent brain lesions as assessed by MRI, including lacunar infarcts. It is therefore plausible to argue that in the absence of lacunar infarcts, the frontal lobe is not especially vulnerable to the damaging effects of CVRF in cognitively

intact individuals. Again, this underscores the topographical similarity between our findings and those reported in previous FDG-PET studies of AD; as such, literature often indicates that frontal lobe regions are spared at early stages of AD.

We also predicted that decreased metabolism in the hippocampal region would be found in proportion to the degree of cardiovascular risk, given both the relevance of this brain region as a critical site of neuropathological AD changes, as well as its particular vulnerability to chronic blood flow deficits in animal models of brain hypoperfusion (Wang et al. 2010; Choi et al. 2011). Rather unexpectedly, we actually found relatively *increased* brain metabolism in a voxel cluster located in the parahippocampal gyrus both in the comparisons across three groups and in the high-risk group when compared to the low-risk group. Moreover, there was a significant positive correlation between CMRgl values and FCHDRP (10-year risk) scores in the parahippocampal gyrus. One possible explanation for the relative hypermetabolism in the parahippocampal gyrus in high CVRF individuals would be a bias in the sample selection. As mentioned above, we excluded participants with silent gross vascular brain lesions detected with MRI, including lacunes and silent strokes, and these lesions were present more frequently in subjects from the high-risk pool of potentially eligible subjects for the present study (de Toledo Ferraz Alves et al. 2011). Therefore, it is possible that we have excluded subjects with severest levels of cardiovascular risk who would have displayed patterns of reduced CMRgl in the parahippocampal gyrus, forcing the selection of individuals who are at high cardiovascular risk but are capable of displaying compensatory mechanisms to maintain adequate metabolic functioning in temporolimbic regions vulnerable to microvascular changes. As suggested previously, subtly damaged neurons may display higher levels of functional activity to maintain their effectiveness, and this could be reflected in a local increment in glucose metabolic rate (Mesulam 1999). Thus, the relative hypermetabolism observed in the parahippocampal gyrus in our study could reflect a very early local response to neurodysfunction, prior to overt cellular structural damage. It is relevant to highlight that in our previous MRI study, we also found a relative increase in gray matter volume involving the parahippocampal gyrus in the high-risk group compared to the low-cardiovascular risk group after the exclusion of subjects with silent brain lesions (de Toledo Ferraz Alves et al. 2011).

The interpretation of the overall results reported herein warrants caution due to a number of limitations of our study. We had an excess of male subjects in the high-risk subgroup, and a larger proportion of women in the low-risk group. This is in consistence with previous epidemiological investigations of vascular risk in elderly populations (Elias et al. 1997; Ishii et al. 2009). Such demographic imbalance has to be highlighted, given the evidence that gender differences clearly influence CMRgl distribution in healthy elderly subjects (Fujimoto et al. 2008; Curiati et al. 2011). However, because we co-varied all our analyses for between-group gender differences, our results are unlikely to simply reflect such gender imbalance across the groups. Moreover, previous literature findings indicate that gender differences influence glucose metabolic patterns most notably in frontal lobe regions, with lower metabolic rate in males relative to females (Baxter et al. 1987; Yoshii et al. 1988; Andreason et al. 1994; Fujimoto et al. 2008). This would potentially lead to reduced prefrontal metabolism in the high-risk group compared to the low-risk group in our study, rather than a sparing of the frontal cortex in high-risk individuals as we found. One other limitation regards to the fact that we excluded individuals with a diagnosis of diabetes mellitus. In subjects with diabetes, there are difficulties in the adherence to the PET procedure guidelines that demand fasting prior to FDG-PET imaging (Vander Borght et al. 2001; Bartenstein et al. 2002). It is well known that hyperglycemia and the lack of appropriate fasting in preparation to FDG-PET examinations may lead to substantial FDG uptake by extra brain tissues (Vander Borght et al. 2001; Bartenstein et al. 2002). This leads to a relative decrement in the FDG uptake inside the brain, often hampering statistical image quality due to decreased signal-to-noise ratio (Vander Borght et al. 2001; Bartenstein et al. 2002). Given our use of such exclusion criterion, the present functional brain deficits related to CVRF can only be claimed to be representative of high-risk elderly samples without a history of diabetes mellitus. Finally, the design of our study prevented us from avoiding a delay of the order of months between the acquisition of the actual FDG-PET images in all study groups, and the previous acquisition of the structural MRI datasets that were used for the partial volume effect correction of PET data. Therefore, it is plausible that our PET findings would have been under-corrected for PVE due to the

time difference between the two imaging acquisitions, in case further atrophic brain changes detectable with morphometric MRI would have occurred during such modest window of time up to the date of FDG-PET imaging.

Conclusion

In conclusion, our identification of brain metabolic deficits in association with CVRF in cognitively intact elderlies, involving brain regions previously shown to be especially vulnerable to AD-related brain changes, reinforce the view that the combination of different CVRF may contribute critically to the development of AD neuropathology. Our findings also reinforce the need for a systematic evaluation of vascular risk factors in any FDG-PET studies of elderly populations, suggesting that inter-individual differences in terms of cardiovascular risk load may account for the often high degree of inter-subject variability of brain metabolic indices in elderly samples. Replication of our findings is warranted in further studies carried out with larger elderly samples, including repeated follow-up FDG-PET examinations aimed at dissecting patterns of progression of the subtle functional brain changes reported herein. Rather than aging, all CVRF are preventable and modifiable. Thus, a greater knowledge about how such factors influence brain functioning in healthy subjects over time may provide important insights for the future development of strategies aimed at delaying or preventing the CVRF-related triggering of AD pathologic brain changes.

Acknowledgments The authors thank Carlos Alberto Melo de Morais for helping with technical support, and Dr. Anna Maria Andrei for helping with cardiological evaluation.

References

Acosta-Cabronero J, Williams GB, Pereira JM, Pengas G, Nestor PJ (2008) The impact of skull-stripping and radio-frequency bias correction on grey-matter segmentation for voxel-based morphometry. NeuroImage 39:1654–1665

Alves TC, Rays J, Fraguas R Jr, Wajngarten M, Meneghetti JC, Prando S et al (2005) Localized cerebral blood flow reductions in patients with heart failure: a study using 99mTc-HMPAO SPECT. J Neuroimaging 15:150–156

Andreason PJ, Zametkin AJ, Guo AC, Baldwin P, Cohen RM (1994) Gender-related differences in regional cerebral glucose metabolism in normal volunteers. Psychiatry Res 51:175–183

Baker LD, Cross DJ, Minoshima S, Belongia D, Watson GS, Craft S (2011) Insulin resistance and Alzheimer-like reductions in regional cerebral glucose metabolism for cognitively normal adults with prediabetes or early type 2 diabetes. Arch Neurol 68:51–57

Bangen KJ, Restom K, Liu TT, Jak AJ, Wierenga CE, Salmon DP et al (2009) Differential age effects on cerebral blood flow and BOLD response to encoding: associations with cognition and stroke risk. Neurobiol Aging 30:1276–1287

Bartenstein P, Asenbaum S, Catafau A, Halldin C, Pilowski L, Pupi A et al (2002) European Association of Nuclear Medicine procedure guidelines for brain imaging using [(18)F]FDG. Eur J Nucl Med Mol Imaging 29:BP43–BP48

Baxter LR Jr, Mazziotta JC, Phelps ME, Selin CE, Guze BH, Fairbanks L (1987) Cerebral glucose metabolic rates in normal human females versus normal males. Psychiatry Res 21:237–245

Bell RD, Deane R, Chow N, Long X, Sagare A, Singh I et al (2009) SRF and myocardin regulate LRP-mediated amyloid-beta clearance in brain vascular cells. Nat Cell Biol 11:143–153

Brett M, Johnsrude IS, Owen AM (2002) The problem of functional localization in the human brain [Review]. Nat Rev Neurosci 3:243–249

Chételat G, Desgranges B, de la Sayette V, Viader F, Berkouk K, Landeau B et al (2003) Dissociating atrophy and hypometabolism impact on episodic memory in mild cognitive impairment. Brain 126:1955–1967

Choi BR, Lee SR, Han JS, Woo SK, Kim KM, Choi DH et al (2011) Synergistic memory impairment through the interaction of chronic cerebral hypoperfusion and amlyloid toxicity in a rat model. Stroke 42:2595–2604

Copeland JR, Dewey ME, Griffiths-Jones HM (1986) A computerized psychiatric diagnostic system and case nomenclature for elderly subjects: GMS and AGECAT. Psychol Med 16:89–99

Corder EH, Saunders AM, Strittmatter WJ, Schmechel DE, Gaskell PC, Small GW et al (1993) Gene dose of apolipoprotein E type 4 allele and the risk of Alzheimer's disease in late onset families. Science 261:921–923

Craft S (2009) The role of metabolic disorders in Alzheimer disease and vascular dementia: two roads converged [Review]. Arch Neurol 66:300–305

Curiati PK, Tamashiro-Duran JH, Duran FL, Buchpiguel CA, Squarzoni P, Romano DC et al (2011) Age-related metabolic profiles in cognitively healthy elders: results from a voxel-based [18F]fluorodeoxyglucose-positron-emission tomography study with partial volume effects correction. AJNR Am J Neuroradiol 32:560–565

de la Torre JC (1999) Critical threshold cerebral hypoperfusion causes Alzheimer's disease? [Review]. Acta Neuropathol 98:1–8

de la Torre JC (2009) Cerebrovascular and cardiovascular pathology in Alzheimer's disease [Review]. Int Rev Neurobiol 84:35–48

de la Torre JC, Mussivand T (1993) Can disturbed brain microcirculation cause Alzheimer's disease? [Review]. Neurol Res 15:146–153

de la Torre JC, Pappas BA, Prevot V, Emmerling MR, Mantione K, Fortin T et al (2003) Hippocampal nitric oxide upregulation precedes memory loss and A beta 1–40 accumulation after chronic brain hypoperfusion in rats. Neurol Res 25:635–641

de Toledo Ferraz Alves TC, Scazufca M, Squarzoni P, de Souza Duran FL, Tamashiro-Duran JH, Vallada HP et al (2011) Subtle gray matter changes in temporo-parietal cortex associated with cardiovascular risk factors. J Alzheimers Dis 27:575–589

Drzezga A, Grimmer T, Riemenschneider M, Lautenschlager N, Siebner H, Alexopoulus P et al (2005) Prediction of individual clinical outcome in MCI by means of genetic assessment and (18)F-FDG PET. J Nucl Med 46:1625–1632

Elias MF, Elias PK, D'Agostino RB, Silbershatz H, Wolf PA (1997) Role of age, education, and gender on cognitive performance in the Framingham Heart Study: community-based norms. Exp Aging Res 23:201–235

Eriksson SH, Thom M, Symms MR, Focke NK, Martinian L, Sisodiya SM et al (2009) Cortical neuronal loss and hippocampal sclerosis are not detected by voxel-based morphometry in individual epilepsy surgery patients. Hum Brain Mapp 30:3351–3360

Erkinjuntti T, Gauthier S (2009) The concept of vascular cognitive impairment [Review]. Front Neurol Neurosci 24:79–85

Faul F, Erdfelder E, Lang AG, Buchner A (2007) G*Power 3: a flexible statistical power analysis program for the social, behavioral, and biomedical sciences. Behav Res Methods 39:175–191

Fitzpatrick AL, Kuller LH, Lopez OL, Diehr P, O'Meara ES, Longstreth WT Jr et al (2009) Midlife and late-life obesity and the risk of dementia: cardiovascular health study. Arch Neurol 66:336–342

Friston KJ, Holmes A, Poline JB, Price CJ, Frith CD (1996) Detecting activations in PET and fMRI: levels of inference and power. NeuroImage 4:223–235

Fujimoto T, Matsumoto T, Fujita S, Takeuchi K, Nakamura K, Mitsuyama Y et al (2008) Changes in glucose metabolism due to aging and gender-related differences in the healthy human brain. Psychiatry Res 164:58–72

Gimbrone MA Jr (1999) Endothelial dysfunction, hemodynamic forces, and atherosclerosis [Review]. Thromb Haemost 82:722–726

Gimbrone MA (2010) The Gordon Wilson lecture. Understanding vascular endothelium: a pilgrim's progress. Endothelial dysfunction, biomechanical forces and the pathobiology of atherosclerosis. Trans Am Clin Climatol Assoc 121:115–127

Gorelick PB (2004) Risk factors for vascular dementia and Alzheimer disease [Review]. Stroke 35:2620–2622

Grammas P (2000) A damaged microcirculation contributes to neuronal cell death in Alzheimer's disease [Review]. Neurobiol Aging 21:199–205

Grammas P (2011) Neurovascular dysfunction, inflammation and endothelial activation: implications for the pathogenesis of Alzheimer's disease. [Review]. J Neuroinflammation 8:26

Grammas P, Martinez J, Miller B (2011) Cerebral microvascular endothelium and the pathogenesis of neurodegenerative diseases. [Review]. Expert Rev Mol Med 13:e19

Irie F, Fitzpatrick AL, Lopez OL, Kuller LH, Peila R, Newman AB et al (2008) Enhanced risk for Alzheimer disease in persons with type 2 diabetes and APOE epsilon4: the Cardiovascular Health Study Cognition Study. Arch Neurol 65:89–93

Ishii H, Ishikawa H, Meguro K, Tashiro M, Yamaguchi S (2009) Decreased cortical glucose metabolism in converters from CDR 0.5 to Alzheimer's disease in a community: the Osaki-Tajiri Project. Int Psychogeriatr 21:148–156

Jagust W (2006) Positron emission tomography and magnetic resonance imaging in the diagnosis and prediction of dementia [Review]. Alzheimers Dement 2:36–42

Jeerakathil T, Wolf PA, Beiser A, Massaro J, Seshadri S, D'Agostino RB et al (2004) Stroke risk profile predicts white matter hyperintensity volume: the Framingham Study. Stroke 35:1857–1861

Kawachi T, Ishii K, Sakamoto S, Sasaki M, Mori T, Yamashita F et al (2006) Comparison of the diagnostic performance of FDG-PET and VBM-MRI in very mild Alzheimer's disease. Eur J Nucl Med Mol Imaging 33:801–809

Kitagawa K (2010) Cerebral blood flow measurement by PET in hypertensive subjects as a marker of cognitive decline [Review]. J Alzheimers Dis 20:855–859

Kivipelto M, Rovio S, Ngandu T, Kareholt I, Eskelinen M, Winblad B et al (2008) Apolipoprotein E epsilon4 magnifies lifestyle risks for dementia: a population-based study. J Cell Mol Med 12:2762–2771

Knopman D, Boland LL, Mosley T, Howard G, Liao D, Szklo M et al (2001) Cardiovascular risk factors and cognitive decline in middle-aged adults. Neurology 56:42–48

Kuczynski B, Jagust W, Chui HC, Reed B (2009) An inverse association of cardiovascular risk and frontal lobe glucose metabolism. Neurology 72:738–743

Kumar-Singh S (2008) Cerebral amyloid angiopathy: pathogenetic mechanisms and link to dense amyloid plaques [Review]. Genes Brain Behav 7:67–82

Langbaum JB, Chen K, Caselli RJ, Lee W, Reschke C, Bandy D et al (2010) Hypometabolism in Alzheimer-affected brain regions in cognitively healthy Latino individuals carrying the apolipoprotein E epsilon4 allele. Arch Neurol 67:462–468

Langbaum JB, Chen K, Launer LJ, Fleisher AS, Lee W, Liu X et al (2012) Blood pressure is associated with higher brain amyloid burden and lower glucose metabolism in healthy late middle-age persons. Neurobiol Aging 33:827.e11–9

Launer LJ, Ross GW, Petrovitch H, Masaki K, Foley D, White LR et al (2000) Midlife blood pressure and dementia: the Honolulu-Asia aging study. Neurobiol Aging 21:49–55

Li J, Wang YJ, Zhang M, Xu ZQ, Gao CY, Fang CQ et al (2011) Vascular risk factors promote conversion from mild cognitive impairment to Alzheimer disease. Neurology 76:1485–1491

Libby P (2009) Molecular and cellular mechanisms of the thrombotic complications of atherosclerosis [Review]. J Lipid Res 50:S352–S357

Massaro JM, D'Agostino RB Sr, Sullivan LM, Beiser A, DeCarli C, Au R et al (2004) Managing and analysing data from a large-scale study on Framingham Offspring relating brain structure to cognitive function. Stat Med 23:351–367

Meigs JB, Singer DE, Sullivan LM, Dukes KA, D'Agostino RB, Nathan DM et al (1997) Metabolic control and prevalent cardiovascular disease in non-insulin-dependent diabetes mellitus (NIDDM): the NIDDM Patient Outcome Research Team. Am J Med 102:38–47

Meltzer CC, Cantwell MN, Greer PJ, Ben-Eliezer D, Smith G, Frank G et al (2000) Does cerebral blood flow decline in

healthy aging? A PET study with partial-volume correction. J Nucl Med 41:1842–1848
Menon U, Kelley RE (2009) Subcortical ischemic cerebrovascular dementia [Review]. Int Rev Neurobiol 84:21–33
Mesulam MM (1999) Neuroplasticity failure in Alzheimer's disease: bridging the gap between plaques and tangles [Review]. Neuron 24:521–529
Meyer JS, Rauch GM, Rauch RA, Haque A, Crawford K (2000) Cardiovascular and other risk factors for Alzheimer's disease and vascular dementia. Ann N Y Acad Sci 903:411–423
Minoshima S, Giordani B, Berent S, Frey KA, Foster NL, Kuhl DE (1997) Metabolic reduction in the posterior cingulate cortex in very early Alzheimer's disease. Ann Neurol 42:85–94
Mosconi L (2005) Brain glucose metabolism in the early and specific diagnosis of Alzheimer's disease. FDG-PET studies in MCI and AD [Review]. Eur J Nucl Med Mol Imaging 32:486–510
Mosconi L, De Santi S, Rusinek H, Convit A, de Leon MJ (2004) Magnetic resonance and PET studies in the early diagnosis of Alzheimer's disease [Review]. Expert Rev Neurother 4:831–849
Mosconi L, Tsui WH, Herholz K, Pupi A, Drzezga A, Lucignani G et al (2008a) Multicenter standardized 18F-FDG PET diagnosis of mild cognitive impairment, Alzheimer's disease, and other dementias. J Nucl Med 49:390–398
Mosconi L, De Santi S, Brys M, Tsui WH, Pirraglia E, Glodzik-Sobanska L et al (2008b) Hypometabolism and altered cerebrospinal fluid markers in normal apolipoprotein E E4 carriers with subjective memory complaints. Biol Psychiatry 63:609–618
Obisesan TO, Obisesan OA, Martins S, Alamgir L, Bond V, Maxwell C et al (2008) High blood pressure, hypertension, and high pulse pressure are associated with poorer cognitive function in persons aged 60 and older: the Third National Health and Nutrition Examination Survey. J Am Geriatr Soc 56:501–509
Pereira JM, Xiong L, Acosta-Cabronero J, Pengas G, Williams GB, Nestor PJ (2010) Registration accuracy for VBM studies varies according to region and degenerative disease grouping. NeuroImage 49:2205–2215
Petrie EC, Cross DJ, Galasko D, Schellenberg GD, Raskind MA, Peskind ER et al (2009) Preclinical evidence of Alzheimer changes: convergent cerebrospinal fluid biomarker and fluorodeoxyglucose positron emission tomography findings. Arch Neurol 66:632–637
Prince M, Ferri CP, Acosta D, Albanese E, Arizaga R, Dewey M et al (2007) The protocols for the 10/66 dementia research group population-based research programme. BMC Publ Health 7:165
Qiu C, Kivipelto M, von Strauss E (2009) Epidemiology of Alzheimer's disease: occurrence, determinants, and strategies toward intervention [Review]. Dialogues Clin Neurosci 11:111–128
Quarantelli M, Berkouk K, Prinster A, Landeau B, Svarer C, Balkay L et al (2004) Integrated software for the analysis of brain PET/SPECT studies with partial-volume-effect correction. J Nucl Med 45:192–201
Razay G, Vreugdenhil A, Wilcock G (2007) The metabolic syndrome and Alzheimer disease. Arch Neurol 64:93–96
Reiman EM, Chen K, Alexander GE, Caselli RJ, Bandy D, Osborne D et al (2004) Functional brain abnormalities in young adults at genetic risk for late-onset Alzheimer's dementia. Proc Natl Acad Sci U S A 101:284–289
Reiman EM, Chen K, Langbaum JB, Lee W, Reschke C, Bandy D et al (2010) Higher serum total cholesterol levels in late middle age are associated with glucose hypometabolism in brain regions affected by Alzheimer's disease and normal aging. NeuroImage 49:169–176
Rosendorff C, Beeri MS, Silverman JM (2007) Cardiovascular risk factors for Alzheimer's disease [Review]. Am J Geriatr Cardiol 16:143–149
Salmina AB, Inzhutova AI, Malinovskaya NA, Petrova MM (2010) Endothelial dysfunction and repair in Alzheimer-type neurodegeneration: neuronal and glial control [Review]. J Alzheimers Dis 22:17–36
Scazufca M, Seabra CA (2008) Sao Paulo portraits: ageing in a large metropolis. Int J Epidemiol 37:721–723
Scazufca M, Menezes PR, Vallada HP, Crepaldi AL, Pastor-Valero M, Coutinho LM et al (2008) High prevalence of dementia among older adults from poor socioeconomic backgrounds in Sao Paulo, Brazil. Int Psychogeriatr 20:394–405
Seshadri S (2006) Methodology for measuring cerebrovascular disease burden [Review]. Int Rev Psychiatry 18:409–422
Seshadri S, Wolf PA, Beiser A, Elias MF, Au R, Kase CS et al (2004) Stroke risk profile, brain volume, and cognitive function: the Framingham Offspring Study. Neurology 63:1591–1599
Smith SM, De Stefano N, Jenkinson M, Matthews PM (2001) Normalized accurate measurement of longitudinal brain change. J Comput Assist Tomogr 25:466–475
Smith SM, Zhang Y, Jenkinson M, Chen J, Matthews PM, Federico A, et al (2002) Accurate, robust, and automated longitudinal and cross-sectional brain change analysis. Neuroimage 17:479–489
Stuerenburg HJ, Ganzer S, Arlt S, Muller-Thomsen T (2005) The influence of smoking on plasma folate and lipoproteins in Alzheimer disease, mild cognitive impairment and depression. Neuro Endocrinol Lett 26:261–263
Talairach J, Tournoux P (1988) Co-planar stereotaxic atlas of the human brain. Thieme Medical, New York
Teipel SJ, Meindl T, Wagner M, Kohl T, Burger K, Reiser MF et al (2009) White matter microstructure in relation to education in aging and Alzheimer's disease. J Alzheimers Dis 17:571–583
Vander Borght T, Laloux P, Maes A, Salmon E, Goethals I, Goldman S (2001) Guidelines for brain radionuclide imaging. Perfusion single photon computed tomography (SPECT) using Tc-99m radiopharmaceuticals and brain metabolism positron emission tomography (PET) using F-18 fluorodeoxyglucose. The Belgian Society for Nuclear Medicine. Acta Neurol Belg 101:196–209
Viswanathan A, Rocca WA, Tzourio C (2009) Vascular risk factors and dementia: how to move forward? [Review]. Neurology 72:368–374
Volkow ND, Wang GJ, Telang F, Fowler JS, Goldstein RZ, Alia-Klein N et al (2009) Inverse association between BMI and prefrontal metabolic activity in healthy adults. Obesity 17:60–65
Wang X, Xing A, Xu C, Cai Q, Liu H, Li L (2010) Cerebrovascular hypoperfusion induces spatial memory impairment,

synaptic changes, and amyloid-beta oligomerization in rats. J Alzheimers Dis 21:813–822

Wilson PW, D'Agostino RB, Levy D, Belanger AM, Silbershatz H, Kannel WB (1998) Prediction of coronary heart disease using risk factor categories. Circulation 97:1837–1847

Xu W, Qiu C, Gatz M, Pedersen NL, Johansson B, Fratiglioni L (2009) Mid- and late-life diabetes in relation to the risk of dementia: a population-based twin study. Diabetes 58:71–77

Yoshii F, Barker WW, Chang JY, Loewenstein D, Apicella A, Smith D et al (1988) Sensitivity of cerebral glucose metabolism to age, gender, brain volume, brain atrophy, and cerebrovascular risk factors. J Cereb Blood Flow Metab 8:654–661

Zlokovic BV (2005) Neurovascular mechanisms of Alzheimer's neurodegeneration [Review]. Trends Neurosci 28:202–208

Zlokovic BV (2010) Neurodegeneration and the neurovascular unit. Nat Med 16:1370–1371

Further Readings

Ashburner J (2007) A fast diffeomorphic image registration algorithm. NeuroImage 38:95–113

Ashburner J, Friston KJ (2005) Unified segmentation. NeuroImage 26:839–851